Antithetical Stratified Sampling Estimator for Filtering Signals with Discontinuities

Darawsheh, H. and Tarczynski, A.

Antithetical Stratified Sampling Estimator for Filtering Signals with Discontinuities

Hikmat Y. Darawsheh, *Student Member, IEEE,* and Andrzej Tarczynski, *Member, IEEE*

***Abstract*—A novel approach to signal filtering using digital alias-free signal processing (DASP) is presented in this paper. We propose an unbiased, fast-converging estimator of the output of a finite impulse response (FIR) continuous-time filter. The estimator processes $2N$ signal samples collected with the use of random antithetical stratified (AnSt) sampling technique. To assess the estimator convergence rate as the function of N, we consider various forms of smoothness of the input signal, filter impulse response and windowing function. The cases are piecewise-continuous second-order derivative (SOD), piecewise-continuous first-order derivative (FOD) and piecewise-continuous zero-order derivative (ZOD). In each case we assume that the respective derivative has a finite number of bounded discontinuities. We prove that the proposed estimator converges to the true filter output at the rate of N^{-5} in the first case. But for the other two the rate drops to N^{-4} and N^{-2} respectively.**

***Index Terms*—Random sampling, filter estimator, uniform convergence rate, antithetical stratification, derivative discontinuities.**

1. Introduction

Sampling of continuous-time functions in classical digital signal processing (DSP) is carried out uniformly. Aliasing problem takes place when the utilized uniform sampling frequency is less than the Nyquist rate [1], [2]. Fortunately, cost-effective sub-Nyquist random sampling techniques have emerged as a promising approach, in digital alias-free signal processing (DASP), that can mitigate this issue [3]–[8]. Numerous publications have then been available exploring different implementations of DASP systems [9]–[13], including random filtering applications and estimators [14]–[21]. In particular, AnSt-based technique has been addressed in [17] to explore filtering of bandlimited randomly sampled signals. However, it does not include any reference to discontinuities that might present in the input signal or its various-order derivatives. The effect of such discontinuities on filtering estimators, including variance and uniform convergence rate, has been introduced in [20], [21] but only for stratified sampling (StSa) technique. StSa is different from AnSt sampling technique in the way the random sampling points are acquired, and in the number of sampling points per each stratum. AnSt technique will be explained in more detail in the next section.

Practically, discontinuities in the ZOD, FOD or SOD of the input signals occur so frequently in everyday applications. For instance, clipping or rectifying of continuous-time signals leads to discontinuities in one or more orders of derivative [22]. Other examples include communication signals, transient signals, power cut and digital data. In stock market field, ZOD, FOD or SOD discontinuities occur in some financial data due to major global events, such as COVID-19 pandemic [23]. Moreover, many smoothing window functions used in filtering also have discontinuities in some orders of the derivative. To name a few: Rectangular, Triangular, Hamming, Tukey and Exponential (Poisson) are all examples of such discontinuous averaging windows.

Theoretically, in classical DSP applications, many mathematical functions, including discontinuous ones, can be used as the impulse response of some given filters. For example, in software-defined radios, digital audio processing, software-based filter design or similar applications, we may use one of the above-mentioned discontinuous windows, or even any generic function, as a filter that suits our application. Therefore, the work in this paper bridges the gap by addressing the implications of such realistic discontinuities on FIR filtering applications while considering AnSt as the utilized random sampling technique.

1.1. *Related Work*

Many applications of DASP have been introduced in [6], [7] including estimation of the Fourier transform (FT) coefficients and filtering of randomly sampled signals. However, such general references neither consider cases where the processed signal has got some discontinuities nor mention anything related to stratification schemes, such as StSa or AnSt. Whereas other papers [9]–[11], [24] focus on spectral estimation of randomly sampled continuous-time signals using either total random (ToRa) sampling technique or StSa. A uniform decay rate of N^{-1} has been proven for the ToRa-based estimator and N^{-3} for the StSa-based one. But then, no discussion about signal filtering or discontinuities have been provided there.

In [25], an estimator based on AnSt technique is used to estimate the FT of a randomly sampled signal. The estimator was proven to be unbiased, and its variance has a uniform

The authors are with the School of Computer Science and Engineering, University of Westminster, London W1W 6UW, UK (e-mails: hikmat.darawsheh@my.westminster.ac.uk; tarczya@westminster.ac.uk).

convergence rate of N^{-5}. However, a fundamental assumption has been made to apply the Taylor series expansion of the input signal properly. The assumption emphasized that the input signal should have continuous ZOD, FOD and SOD across the whole observation window, which is a necessary and sufficient condition for expanding functions to second-degree polynomials using Taylor series. In addition, [25] has not addressed the filtering case.

The works in [20], [21] particularly, have presented discussions about the statistical properties of an FIR filter estimator that utilises StSa technique with the presence of discontinuities in the input signal or its FOD. Uniform convergence rates of N^{-2} and N^{-3} are proven for the filter estimator in these two cases, respectively.

1.2. *Contributions*

The main contributions of this paper are: a) introduction of AnSt random sampling technique to estimate FIR filtering analytically and numerically; b) the study of the effects of discontinuities in the input signal, the window function or the impulse response on the filter estimator, including: 1) devising mathematical expressions for the estimator variance in three considered cases related to the order of the derivative at which the discontinuities occur; 2) rigorously deriving the uniform convergence rates of the filter estimator in those cases.

The reminder of this paper comprises five sections: the next section introduces the AnSt sampling technique. The filter estimator is introduced in Section 3. Whereas, the core of this paper is presented in Section 4, which includes all the mathematical derivations, statistical properties, and related discussion of the filter estimator. Several numerical examples are provided in Section 5 to verify the analytical results. Finally, the conclusion section summarises the main findings of this paper.

2. Background: Antithetical Stratified Sampling

The AnSt random sampling technique depends on the notion of stratification of an observation window. The window time interval, $[0, T]$, is divided into N sub-intervals called strata. Subsequently, two sampling points are acquired per each stratum, as shown in Fig. 1. The first sampling point of the j-th stratum, τ_j, is selected randomly using a probability density function uniformly distributed within the stratum's time span. The second one is its antithetical counterpart and is given by $\tau_j^A = 2C_j - \tau_j$, where C_j is the centre of the stratum. The process of selecting strata lengths is detailed in [24], [25]. Indeed, one of its simplest forms is to divide the whole observation window equidistantly. While this is not necessarily the optimum way of portioning and it is possible to improve estimation by choosing different arrangement, however, this greatly depends on a priori knowledge of the sampled signal. For example, we may have more strata concentrated around steep slopes of the sampled signal. But in this paper, we assume that the sampled signal is not known in advance, therefore, we choose the first stratification setup, where all strata are of equal lengths, i.e. the stratum length is T/N.

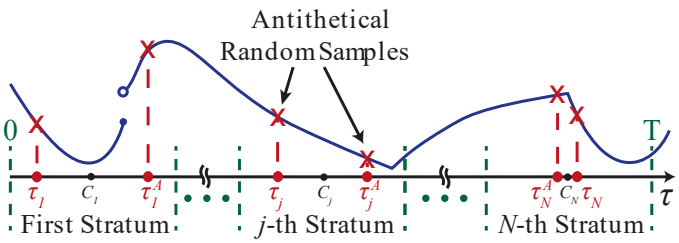

Fig. 1. In AnSt technique, two sampling points are acquired per each stratum. The time instant of the first point, τ_j, is randomly selected within the stratum, while the time instant of the other one, τ_j^A, is its antithetical counterpart. τ_j is chosen based on a uniformly distributed random process.

3. The Filter Estimator

Consider an LTI causal filter with an impulse response $h(t)$, input signal $x(t)$, window function $w(t)$ defined over the interval $[0, T]$. The windowed output signal $y(t)$ is given by

$$y(t) = \int_0^T x(\tau)w(\tau)h(t-\tau)d\tau. \tag{1}$$

We define the integrated function in (1) as $g(t, \tau)$,

$$g(t, \tau) := x(\tau)w(\tau)h(t-\tau). \tag{2}$$

If $g(t, \tau)$ has continuous SOD within the observation window then, as we show later, the uniform convergence rate of the estimator proposed here is exactly N^{-5}, where N is the total number of strata within the window interval. This rate is similar to the one in [25] but for another application, i.e. the FT. However, if $g(t, \tau)$ has some bounded discontinuities in the SOD then the approach in [25] is not valid, since the main condition for applying Taylor series expansion is not satisfied. In this paper, we thoroughly explore cases when any of SOD, FOD or ZOD of the integrated function $g(t, \tau)$, has a finite number of discontinuities.

We propose a filter estimator, $\hat{y}(t)$, which approximates the output $y(t)$ using N independent and identically distributed (i.i.d) stratified random sampling points, along with their N antithetical counterparts. The estimator is defined by

$$\hat{y}(t) := \sum_{j=1}^{N} \left(g(t, \tau_j) + g(t, \tau_j^A) \right) \frac{\Delta_j}{2}, \tag{3}$$

where Δ_j is the length of the j-th stratum (for equidistant strata, $\Delta_j = T/N := \Delta$), and τ_j and τ_j^A are the time instants of the j-th antithetical sampling pair. The probability density functions (PDFs) of τ_j and τ_j^A are the same, and they are equal to $p_j(\tau_j) = 1/\Delta_j$ within the j-th stratum and zero elsewhere.

We start the analysis by establishing Theorem 1, which determines one of the statistical properties of the estimator, (i.e. the unbiasedness). The proof of this theorem is presented in Appendix A, which depends on the notation illustrated in Fig. 2 and listed in Table I.

Theorem 1. *The AnSt-based filter estimator, defined in (3), is unbiased for any t.*

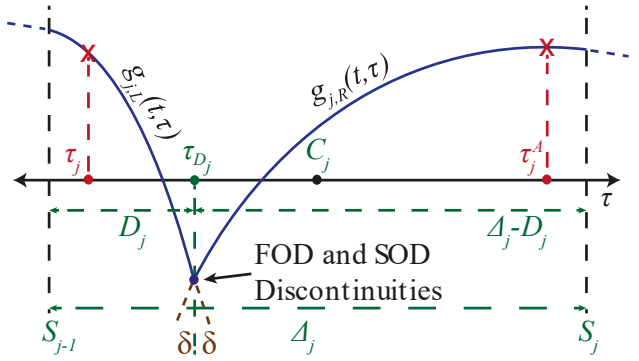

Fig. 2. The j-th stratum of the integrated function, $g(t,\tau)$, having SOD and FOD discontinuities at time instant τ_{D_j}. Remark the left- and right-hand pieces $g_{j,L}(t,\tau)$ and $g_{j,R}(t,\tau)$, respectively, alongside other notation.

TABLE I
Notation as Per The j-th Stratum

Δ_j	The length of the j-th stratum (= Δ for equal strata)
S_{j-1}	The start time of the j-th stratum, with $S_0 = 0$.
S_j	The end time of the j-th stratum, with $S_N = T$.
C_j	The central time of the j-th stratum = $(S_{j-1} + S_j)/2$.
τ_{D_j}	The time instant in the j-th stratum at which there is a discontinuity in one or more derivatives of $g(t,\tau)$.
$A_{j,L}$	The j-th stratum left subinterval, $[S_{j-1}, \tau_{D_j})$.
$A_{j,R}$	The j-th stratum right subinterval, $[\tau_{D_j}, S_j)$.
D_j	The time length of $A_{j,L}$, where $g_{j,L}(t,\tau)$ is exactly matching the left part of $g(t,\tau)$ in the j-th stratum. i.e. $D_j = \tau_{D_j} - S_{j-1}$.
$\Delta_j - D_j$	The time length of $A_{j,R}$, where $g_{j,R}(t,\tau)$ is exactly matching the right part of $g(t,\tau)$ in the j-th stratum.
τ_j	The random time instant of the j-th sampling point.
τ_j^A	The antithetical counterpart of τ_j, i.e. $\tau_j^A = 2C_j - \tau_j$.
K_j	The ratio D_j/Δ_j, i.e. the ratio of the time length from the beginning of the stratum to the discontinuity point to the whole length of the stratum, Therefore, $0 \le K_j \le 1$.

As per the result of Theorem 1, the variance of the estimator is equivalent to its mean-squared error (MSE). In the following sub-sections, we investigate the variance of the estimator in the presence of discontinuities in the integrated function. But first, we introduce a generic j-th stratum within which $g(t,\tau)$ has got some discontinuities. We assume that the number of strata is sufficiently large (or equivalently the stratum length is sufficiently small) so that within any stratum there is no more than one discontinuity in the SOD, FOD or ZOD.

Fig. 2 depicts the j-th stratum of an integrated function with SOD and FOD discontinuities located at the time instant τ_{D_j}. Two SOD-continuous sub-functions, $g_{j,L}(t,\tau)$ and $g_{j,R}(t,\tau)$, are now defined per each stratum such that,

$$g_{j,L}(t,\tau) := \begin{cases} g(t,\tau), & \tau \in A_{j,L} \\ g_{j,xL2R}(t,\tau), & \tau_{D_j} \le \tau \le \tau_{D_j} + \delta \end{cases}, \quad (4a)$$

$$g_{j,R}(t,\tau) := \begin{cases} g(t,\tau), & \tau \in A_{j,R} \\ g_{j,xR2L}(t,\tau), & \tau_{D_j} - \delta \le \tau < \tau_{D_j} \end{cases}, \quad (4b)$$

where $g_{j,xL2R}(t,\tau)$ and $g_{j,xR2L}(t,\tau)$ are extrapolated extensions of the left- and right-hand parts of $g(t,\tau)$, in the j-th stratum, respectively, to δ-wide neighbourhoods of the discontinuity point, τ_{D_j}. And δ is a sufficiently large period of time that ensures the SOD continuity of both $g_{j,L}(t,\tau)$ and $g_{j,R}(t,\tau)$ sub-functions about τ_{D_j}. Therefore, the integrated function can be represented by both sub-functions, across the whole observation window, as

$$g(t,\tau) = \sum_{j=1}^{N} \begin{cases} g_{j,L}(t,\tau), & \tau \in A_{j,L} \\ g_{j,R}(t,\tau), & \tau \in A_{j,R} \end{cases}. \quad (5)$$

Since these sub-functions are continuous to the order of the second derivative and sufficiently extended to the neighbourhoods of τ_{D_j}, they can be approximated individually by a second-degree polynomial using Taylor series expansion. Indeed, we conduct such expansion about the discontinuity point itself, as indicated in (10a) of the next section.

From now on, we drop the time shift parameter, t, from all functions and equations for the sake of simplicity and to save paper space, unless it is necessary to show it explicitly. Let the notation "≡" denote equivalence, then we have $g(\tau) \equiv g(t,\tau)$, $g_{j,L}(\tau) \equiv g_{j,L}(t,\tau)$, $g_{j,R}(\tau) \equiv g_{j,R}(t,\tau)$, $\hat{y} \equiv \hat{y}(t)$ and so on. Δ will replace Δ_j, as we assume all strata to be equidistant.

4. Discontinuities in the Integrated Function

The implications of the presence of discontinuities, in the integrated function, for the filter estimator vary according to the order of the derivative at which these discontinuities are existing. Let the differences between the left and right edges of the SOD, FOD and ZOD discontinuities (i.e. the amplitudes of the jumps) in the j-th stratum be defined as G_{2j}, G_{1j} and G_{0j}, respectively. Then, we have

$$G_{2j} := g''_{j,L}\left(\tau_{D_j}\right) - g''_{j,R}\left(\tau_{D_j}\right). \quad (6a)$$

$$G_{1j} := g'_{j,L}\left(\tau_{D_j}\right) - g'_{j,R}\left(\tau_{D_j}\right). \quad (6b)$$

$$G_{0j} := g_{j,L}\left(\tau_{D_j}\right) - g_{j,R}\left(\tau_{D_j}\right). \quad (6c)$$

In the following sub-sections, we consider three main cases for the order of discontinuities in the integrated function: either

they present in the SOD, FOD or ZOD.

4.1. *Second-Order Derivative Discontinuities*

Suppose that there is a finite number (e.g. M) of bounded discontinuities in the SOD of the integrated function. Whereas neither FOD nor ZOD discontinuities exist. Assume the SOD discontinuities occur at time instants $\{\tau_{D_j}\}$ where j is a positive index integer less than or equal to M. Hence, the following equations are valid,

$$g_{j,L}\left(\tau_{D_j}\right) = g_{j,R}\left(\tau_{D_j}\right) = g\left(\tau_{D_j}\right), \tag{7a}$$

$$g'_{j,L}\left(\tau_{D_j}\right) = g'_{j,R}\left(\tau_{D_j}\right) = g'\left(\tau_{D_j}\right), \tag{7b}$$

$$g''_{j,L}\left(\tau_{D_j}\right) \neq g''_{j,R}\left(\tau_{D_j}\right). \tag{7c}$$

This means that $G_{1j} = G_{2j} = 0$, whereas $G_{2j} \neq 0$ in this case. To devise a mathematical expression for the variance and find the uniform convergence rate, we adopt the same approach as in [25], this makes it easy for comparison purposes.

Let Z_j be the sub-estimator related to the j-th stratum, thus

$$Z_j = \frac{1}{2}\left(g(\tau_j) + g(\tau_j^A)\right)\Delta \tag{8a}$$

$$Z_j = \frac{\Delta}{2}\begin{Bmatrix} g_{j,L}(\tau_j), & \tau_j \in A_{j,L} \\ g_{j,R}(\tau_j), & \tau_j \in A_{j,R} \end{Bmatrix} + \frac{\Delta}{2}\begin{Bmatrix} g_{j,L}(\tau_j^A), & \tau_j^A \in A_{j,L} \\ g_{j,R}(\tau_j^A), & \tau_j^A \in A_{j,R} \end{Bmatrix} \tag{8b}$$

$$Z_j = \frac{\Delta}{2}\begin{Bmatrix} g_{j,L}(\tau_j) + g_{j,L}(\tau_j^A), & \tau_j \text{ and } \tau_j^A \in A_{j,L} \\ g_{j,L}(\tau_j) + g_{j,R}(\tau_j^A), & \tau_j \in A_{j,L} \text{ and } \tau_j^A \in A_{j,R} \\ g_{j,R}(\tau_j) + g_{j,L}(\tau_j^A), & \tau_j \in A_{j,R} \text{ and } \tau_j^A \in A_{j,L} \\ g_{j,R}(\tau_j) + g_{j,R}(\tau_j^A), & \tau_j \text{ and } \tau_j^A \in A_{j,R} \end{Bmatrix} \tag{8c}$$

The expected value of Z_j is

$$\begin{aligned} E[Z_j] &= \frac{1}{2}\int_{-\infty}^{\infty} p_j(\tau)\left(g(\tau) + g(\tau^A)\right)\Delta\, d\tau \\ &= \frac{1}{2}\int_{S_{j-1}}^{S_j} g(\tau)d\tau + \frac{1}{2}\int_{S_{j-1}}^{S_j} g(\tau^A)d\tau, \end{aligned} \tag{9a}$$

$$\begin{aligned} E[Z_j] &= \frac{1}{2}\int_{A_{j,L}} g_{j,L}(\tau)d\tau + \frac{1}{2}\int_{A_{j,R}} g_{j,R}(\tau)d\tau \\ &+ \frac{1}{2}\int_{A_{j,L}} g_{j,L}(\tau^A)d\tau^A + \frac{1}{2}\int_{A_{j,R}} g_{j,R}(\tau^A)d\tau^A. \end{aligned} \tag{9b}$$

Using Taylor series to expand $g_{j,L}(\tau)$, $g_{j,R}(\tau)$, $g_{j,L}(\tau^A)$ and $g_{j,R}(\tau^A)$ about τ_{D_j}, equation (9b) can be rewritten as

$$\begin{aligned} &E[Z_j] \\ &= \frac{1}{2}\int_{A_{j,L}} \left(g_{j,L}\left(\tau_{D_j}\right) + \left(\tau - \tau_{D_j}\right)g'_{j,L}\left(\tau_{D_j}\right)\right. \\ &\left. + \frac{1}{2}\left(\tau - \tau_{D_j}\right)^2 g''_{j,L}\left(\tau_{D_j}\right) + o\left(\left|\tau - \tau_{D_j}\right|^2\right)\right)d\tau \\ &+ \frac{1}{2}\int_{A_{j,R}} \left(g_{j,R}\left(\tau_{D_j}\right) + \left(\tau - \tau_{D_j}\right)g'_{j,R}\left(\tau_{D_j}\right)\right. \\ &\left. + \frac{1}{2}\left(\tau - \tau_{D_j}\right)^2 g''_{j,R}\left(\tau_{D_j}\right) + o\left(\left|\tau - \tau_{D_j}\right|^2\right)\right)d\tau \\ &+ \frac{1}{2}\int_{A_{j,L}} \left(g_{j,L}\left(\tau_{D_j}\right) + \left(\tau^A - \tau_{D_j}\right)g'_{j,L}\left(\tau_{D_j}\right)\right. \\ &\left. + \frac{1}{2}\left(\tau^A - \tau_{D_j}\right)^2 g''_{j,L}\left(\tau_{D_j}\right) + o\left(\left|\tau^A - \tau_{D_j}\right|^2\right)\right)d\tau^A \\ &+ \frac{1}{2}\int_{A_{j,R}} \left(g_{j,R}\left(\tau_{D_j}\right) + \left(\tau^A - \tau_{D_j}\right)g'_{j,R}\left(\tau_{D_j}\right)\right. \\ &\left. + \frac{1}{2}\left(\tau^A - \tau_{D_j}\right)^2 g''_{j,R}\left(\tau_{D_j}\right) + o\left(\left|\tau^A - \tau_{D_j}\right|^2\right)\right)d\tau^A, \end{aligned} \tag{10a}$$

$$\begin{aligned} &E[Z_j] \\ &= \frac{1}{6}\left(K_j^3 g''_{j,L}\left(\tau_{D_j}\right) - \left(K_j^3 - 3K_j^2 + 3K_j - 1\right)g''_{j,R}\left(\tau_{D_j}\right)\right)\Delta^3 \\ &+ \frac{1}{2}(1 - 2K_j)g'_{j,R}\left(\tau_{D_j}\right)\Delta^2 + g_{j,R}\left(\tau_{D_j}\right)\Delta + o(\Delta^3). \end{aligned} \tag{10b}$$

Remark that (10b) is the result of the integration in (10a) after working out the algebra and taking (7a)-(7c) into consideration. The estimator error associated with the j-th stratum is defined by $e_j := Z_j - E[Z_j]$. So, we have from (8b) and (10b)

$$\begin{aligned} e_j = {} & \frac{\Delta}{2}\left(\begin{Bmatrix} g_{j,L}(\tau_j), & \tau_j \in A_{j,L} \\ g_{j,R}(\tau_j), & \tau_j \in A_{j,R} \end{Bmatrix} + \begin{Bmatrix} g_{j,L}(\tau_j^A), & \tau_j^A \in A_{j,L} \\ g_{j,R}(\tau_j^A), & \tau_j^A \in A_{j,R} \end{Bmatrix}\right) - \\ & \left(\frac{1}{6}\left(K_j^3 g''_{j,L}\left(\tau_{D_j}\right) - c_{1j}g''_{j,R}\left(\tau_{D_j}\right)\right)\Delta^3 + \right. \\ & \left. c_{2j}g'_{j,R}\left(\tau_{D_j}\right)\Delta^2 + g_{j,R}\left(\tau_{D_j}\right)\Delta\right) + o(\Delta^3). \end{aligned} \tag{11}$$

where $c_{1j} = K_j^3 - 3K_j^2 + 3K_j - 1$ and $c_{2j} = \left(1 - 2K_j\right)/2$.

The exact value of e_j in (11) depends on the location of the SOD discontinuity with respect to the two antithetical sampling points of the j-th stratum, τ_j and τ_j^A. Excluding the stratum's centre and border limits, we end up with four possible results for e_j. However, they are similar regarding their effect on the estimator convergence rate, since they all have the same power terms of Δ, and the differences are only on some of the constant coefficients. To save paper space, we consider here one case only, that is when the SOD discontinuity is located between the two antithetical sampling points, i.e. $\tau_j < \tau_{D_j} < \tau_j^A$,

$$\begin{aligned} &e_j \\ &= \frac{1}{4}\left(g''_{j,L}\left(\tau_{D_j}\right) + g''_{j,R}\left(\tau_{D_j}\right)\right)\left(\tau_j - \tau_{D_j}\right)^2\Delta \\ &- c_{2j}\, g''_{j,R}\left(\tau_{D_j}\right)\left(\tau_j - \tau_{D_j}\right)\Delta^2 \\ &+ \frac{1}{12}\left(c_{3j}g''_{j,R}\left(\tau_{D_j}\right) - 2K_j^3 g''_{j,L}\left(\tau_{D_j}\right)\right)\Delta^3 + o(\Delta^3) \end{aligned} \tag{12}$$

where $c_{3j} = 1 - 6K_j + 6K_j^2 + 2K_j^3$.

The variance of the estimator for the j-th stratum, $Var[Z_j]$, is calculated by finding the second moment of e_j,

$$Var[Z_j] = \int_{-\infty}^{\infty} p_j(\tau)\left|e_j\right|^2 d\tau. \tag{13}$$

We now establish the following theorem for the variance of the AnSt-based filter estimator. For the proof, see Appendix B.

Theorem 2. *Assume that $g(\tau)$ is a real-valued and continuous function, and so is its FOD, across an observation window, $[0,T]$, while the SOD has a finite number, M, of bounded discontinuities within the same window. Then, the variance of the N-strata AnSt-based filter estimator, $Var[\hat{y}]$, converges uniformly at a rate of N^{-5} and satisfies*

$$\lim_{N\to\infty} N^5 (Var[\hat{y}]) = \frac{T^5}{720} \sum_{k=1}^{M+1} \int_{T_{k-1}}^{T_k} \left(g''(\tau)\right)^2 d\tau. \tag{14}$$

where $\{T_k\}_{k=1}^{M}$ is a set of time instants at which the SOD is discontinuous, with $T_0 := 0$ and $T_{M+1} := T$.

Based on the results of Theorem 2, it is obvious that the uniform convergence rate of the estimator, N^{-5}, is also applicable when there are no SOD discontinuities at all, since M, in this case, will be zero and (14) reduces to

$$\lim_{N\to\infty} N^5 (Var[\hat{y}]) = \frac{T^5}{720} \int_{0}^{T} \left(g''(\tau)\right)^2 d\tau. \tag{15}$$

4.2. *First-Order Derivative Discontinuities*

If the integrated function is continuous but not its FOD and SOD, rather, they are discontinuous at some τ_{D_j} points, then

$$g_{j,L}\left(\tau_{D_j}\right) = g_{j,R}\left(\tau_{D_j}\right) = g\left(\tau_{D_j}\right), \tag{16a}$$

$$g'_{j,L}\left(\tau_{D_j}\right) \neq g'_{j,R}\left(\tau_{D_j}\right), \tag{16b}$$

$$g''_{j,L}\left(\tau_{D_j}\right) \neq g''_{j,R}\left(\tau_{D_j}\right). \tag{16c}$$

The impact of such discontinuities on the filter estimator is reflected on its variance and uniform convergence rate. The following theorem shows an exact expression for the variance that we have obtained. The proof is shown in Appendix C.

Theorem 3. *Assume that $g(\tau)$ is a real-valued continuous function, while its FOD and SOD are bounded and discontinuous at a limited number, M, of time instants, $\{\tau_{D_j}\}_{j=1}^{M}$. Then the variance of the AnSt-based filter estimator converges uniformly at a rate of N^{-4} and satisfies*

$$\lim_{N\to\infty} N^4 (Var[\hat{y}(t)]) = \frac{T^4}{12} \sum_{j\in I_M} c_{5j}\, {G_{1j}}^2, \tag{17}$$

where $c_{5j} = 1 - 3\,K_j + 6\,K_j^2 - 6\,K_j^3 + 3\,K_j^4$ and I_M is a set of integers representing strata indices, i.e. $I_M = \{i_1, i_2, i_3, \dots, i_M\}$, at which the discontinuities do occur.

Additionally, we can conclude from the proof of Theorem 3 that a faster convergence rate of N^{-5} should be achieved if all G_{1j}'s are precisely zeros, i.e. no FOD discontinuities at all, which is the same conclusion for the case discussed in the previous sub-section.

4.3. *Zero-Order Derivative Discontinuities*

In this sub-section, we discuss the case where the integrated function itself is discontinuous. Suppose there is a finite number, M, of bounded ZOD discontinuities at some time instants, τ_{D_j}'s, and so are the FOD and SOD. Hence, for any j-th stratum having such discontinuities, we have

$$g_{j,L}\left(\tau_{D_j}\right) \neq g_{j,R}\left(\tau_{D_j}\right) \tag{18a}$$

$$g'_{j,L}\left(\tau_{D_j}\right) \neq g'_{j,R}\left(\tau_{D_j}\right) \tag{18b}$$

$$g''_{j,L}\left(\tau_{D_j}\right) \neq g''_{j,R}\left(\tau_{D_j}\right). \tag{18c}$$

Theorem 4 concludes our findings in this case. The proof of this theorem is given in Appendix D.

Theorem 4. *Assume that $I_M = \{i_1, i_2, i_3, \dots, i_M\}$ is a set of integers denoting the indices of the strata which include ZOD discontinuities of $g(\tau)$. Additionally, assume that these discontinuities are bounded in magnitude. Then the rate of uniform convergence of the AnSt-based filter estimator is exactly N^{-2} and satisfies*

$$\lim_{N\to\infty} N^2 (Var[\hat{y}(t)]) = T^2 \sum_{j\in I_M} {c_{2j}}^2\, {G_{0j}}^2, \tag{19}$$

Furthermore, if there are no ZOD discontinuities at all, i.e. $G_{0j} = 0$ for all values of j, then the proof of Theorem 4 clearly indicates that the uniform convergence rate will exactly be N^{-4}. In addition, a faster rate, N^{-5}, will be achieved if also $G_{1j} = 0$ for all j values, which means no FOD discontinuities present at all. The last two conclusions for the convergence rate match the results demonstrated in the previous two sub-sections.

Remark that the results of Theorems 2-4 suggest that the abstract values of the variance of the filter estimator depend on the number, the locations and the amplitudes of the discontinuities, in each case. Though, the key purpose of this paper is not identifying or eliminating such discontinuities, rather, it introduces an approach of employing antithetical random stratification technique to estimate an FIR filter output in some considered cases of the input signal. Our main interest is to prove the unbiasedness of the estimator, and to find how fast the uniform convergence rates of the estimator will be in those special cases (i.e. presence of discontinuities in different orders of the derivative.) According to the results of these theorems and even if there are no discontinuities at all, there is still a necessity for a priori knowledge of the SOD of the input signal, as indicated in (15), to determine the values of the estimator's variance. Indeed, this is not the case in most practical applications, because if $g''(\tau)$ is known in advance why we would need to sample the signal in the first place. Therefore, this work is not about using the specific values of the

estimator's variance in practical applications, yet it gives a general impression about what to expect regarding the amount of errors if the special considered cases are met. For the usability of the already derived variance expressions in real life applications, we will consider this very topic in a future publication, where the main focus will be on how to enhance the estimator's performance and reduce the values of the variance in different cases. Essentially, this requires from us to employ special techniques that can predict, detect and supress the discontinuities in the integrated function.

5. Numerical Results

To verify our mathematical derivation of the estimator uniform convergence rates, we conduct two sets of numerical examples. In the first set, we only consider abstract functions which either have no discontinuities at all or have a finite number of bounded discontinuities. We approximate the integrals of such functions using AnSt-based estimator and compare the results with the actual integral values within an observation window [0,1.2] sec. Whereas the second set of examples include more practical AnSt-based estimator applications using a lowpass filter and input signals characterize functions with some discontinuities in their ZOD, FOD or SOD.

Consider the theoretical (i.e. abstract) functions

$$g_1(t) = sin(3.4\pi t) - 1.3\,cos(5.8\pi t), \tag{20a}$$

$$g_2(t) = 0.1sin(3.4\pi t) + (t-0.11)|t-0.11| + 1.7(t-0.22)|t-0.22| - 2.9(t-0.33)|t-0.33|, \tag{20b}$$

$$g_3(t) = -7cos(5.8\pi t) + 10S(8.4\pi(t-0.25),0.5), \tag{20c}$$

$$g_4(t) = -7\,cos(5.8\pi t) + 10S(17.7\pi(t-0.95),0), \tag{20d}$$

where $S(t,m)$ is the MATLAB's built-in *sawtooth* function. When m is 0 or 1, S is equivalent to the standard *frac* function, with $frac(t) = t - \lfloor t \rfloor$, where $\lfloor . \rfloor$ denotes the *floor* function. Whereas, if $0 < m < 1$, then S represents the *triangle* wave function $triangle(t) = 2/\pi \times arcsin(sin(t))$. In MATLAB, the *sawtooth* function is implemented in such a way that selects between the two function forms (*frac* or *triangle*) according to the variable m, which also determines where the maximum of the function is. Note that $g_1(t)$ has no discontinuities at all, $g_2(t)$ has some bounded discontinuities which present in the SOD, but not in the FOD or ZOD, $g_3(t)$ is a continuous function while its FOD and SOD are not, and $g_4(t)$ has finite and bounded ZOD discontinuities. Figs. 3-6 show the plots of the functions alongside with the associated AnSt-based estimator's MSEs (variances).

In these AnSt-based estimation examples, we have carried out 64 independent Monte Carlo simulations per each example. This ensures that the outcome is smooth and reliable. It is seen that the uniform convergence rates of the AnSt-based estimator are in $o(N^{-5})$, $o(N^{-5})$, $o(N^{-4})$, and $o(N^{-2})$ for the abstract functions $g_1(t)$, $g_2(t)$, $g_3(t)$, and $g_4(t)$, respectively. These results confirm the analytical findings established in Section 3.

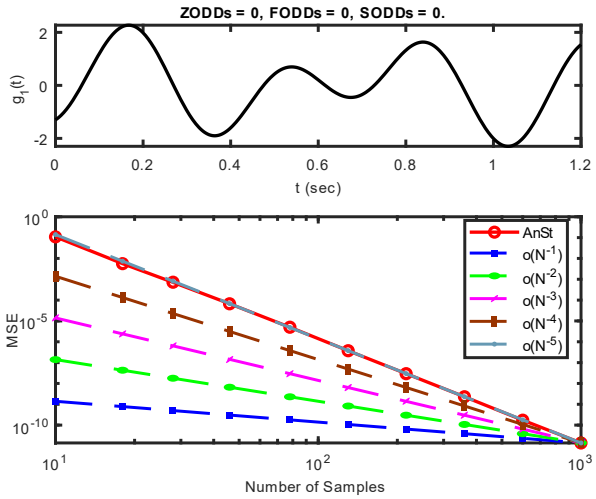

Fig. 3. The function $g_1(t)$ is continuous, and so are all its derivatives. The AnSt-based estimator's uniform convergence rate is N^{-5}.

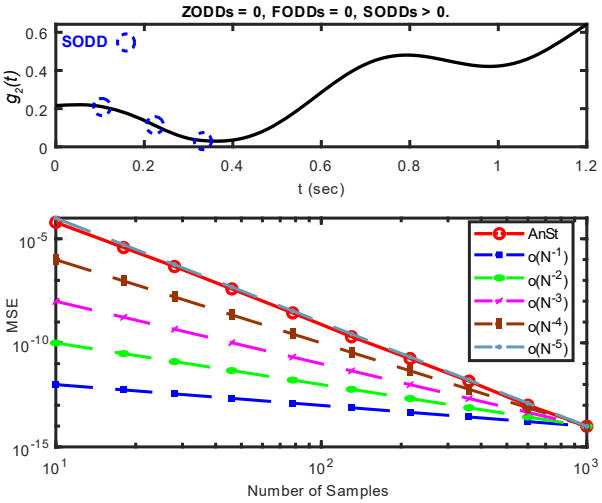

Fig. 4. The function $g_2(t)$ is continuous, and so is its FOD, while there are some bounded discontinuities in the SOD. Though, the AnSt-based estimator's uniform convergence rate is N^{-5}, as well.

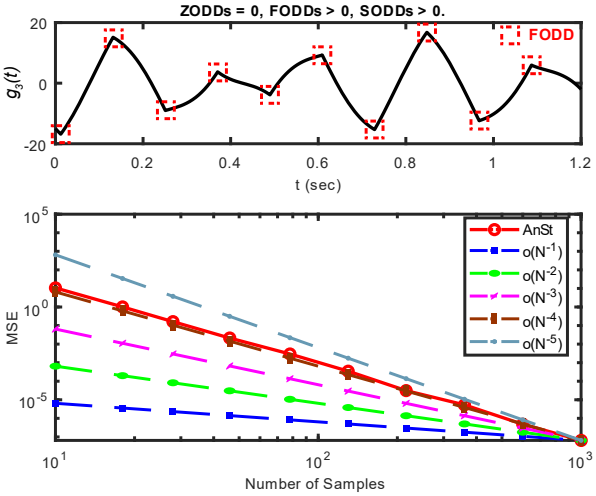

Fig. 5. The function $g_3(t)$ is continuous, but neither its FOD nor SOD is continuous. Therefore, the AnSt-based estimator converges uniformly at a slower rate of N^{-4}.

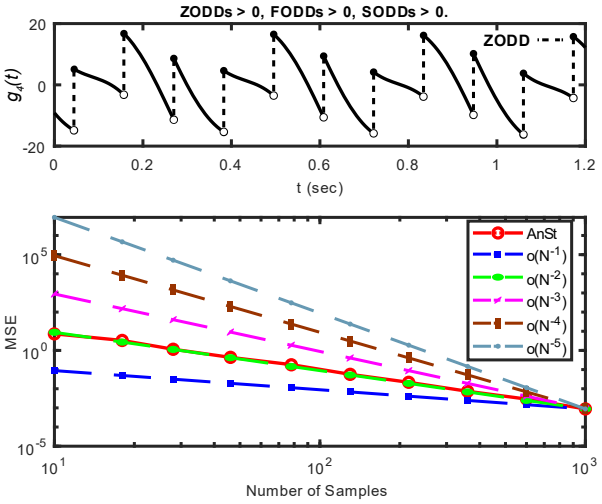

Fig. 6. The function $g_4(t)$ is discontinuous, and so are its FOD and SOD. The AnSt-based estimator converges uniformly at the slowest rate of N^{-2}.

On the other hand, a lowpass filter (LPF) with a cutoff frequency of 13kHz has been designed to check the effectiveness of our AnSt-based filter estimator. The input signals to the filter are sampled uniformly and randomly before the output results got compared. Four input signals have been considered: 1) continuous (no derivative discontinuities at any order); 2) continuous ZOD and FOD but not the SOD; 3) continuous ZOD with finite and bounded FOD and SOD discontinuities, and finally; 4) discontinuous (all orders of derivative). Fig. 7 shows the filter frequency response and the single-sided spectrum of a continuous input signal with no derivative discontinuities at all, whereas Figs. 8-11 depicts the single-sided spectra of the output signals (uniformly and randomly sampled). Observe how much the output spectra of the randomly sampled signals are close to those of the uniformly sampled ones even though the average random sampling frequency is only F_{ARS}=65.536kHz. In contrast, we would need a uniform sampling frequency of at least 126kHz, without using a pre-anti-aliasing filter, to avoid aliasing problem. In our examples, an actual uniform sampling rate of F_{US}=131.072kHz has been used.

Remark that the spectrum errors of the AnSt-based filter estimator in Figs. 8-11 become larger as discontinuities present in the lower orders of derivative, i.e. error amounts increase when moving from Fig. 8 to Fig. 11. While in Fig. 12, the average random sampling frequency is only F_{ARS} =32.768kHz, i.e. one quarter of the total uniform sampling rate. Although the input signal in Fig. 12 has no discontinuities at all, the errors seem to be the maximum here. This is because of the nature of the AnSt-based estimator, which has a fast uniform convergence rate of N^{-5}, in this case. Meaning, the smaller number of sampling points are used, the much more amount of errors appears.

As already indicated for the previous set of examples, the second set of filter estimator numerical examples has been carried out by averaging 128 independent Monte Carlo runs, and not based on a single realisation. This ensures that the findings shown in Figs. 8-12 are confident and rules out the possibility that they are due to a particular sampling sequence.

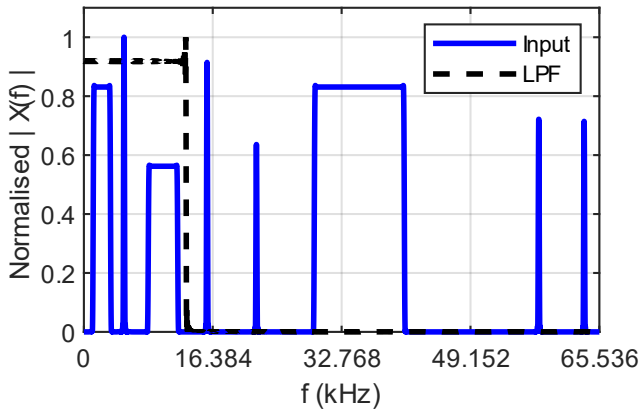

Fig. 7. Frequency response of the 13kHz-bandwidth LPF (dashed black), and spectrum of one of the continuous-time input signals (solid blue) with no derivative discontinuities at any order.

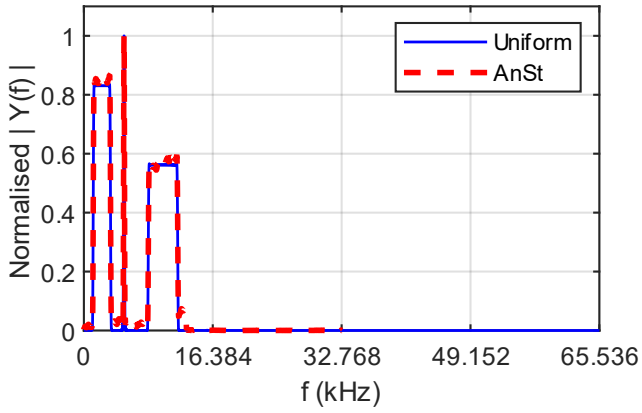

Fig. 8. The spectra of the filter outputs based on uniformly sampled (blue) and AnSt randomly sampled (dashed red) signals. Case 1) the filter input is a continuous-time signal with no derivative discontinuities at any order (see Fig. 7 above.) Uniform sampling frequency is F_{US}=131.072kHz, whereas the average random sampling frequency is F_{ARS}=65.536kHz.

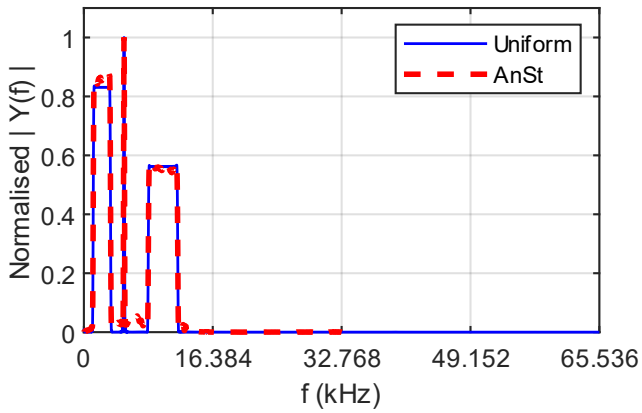

Fig. 9. The spectra of the filter outputs based on uniformly sampled (blue) and AnSt randomly sampled (dashed red) signals. Case 2) the filter input is a continuous-time signal with only 6 bounded SOD discontinuities. F_{US}=131.072kHz, whereas F_{ARS}=65.536kHz.

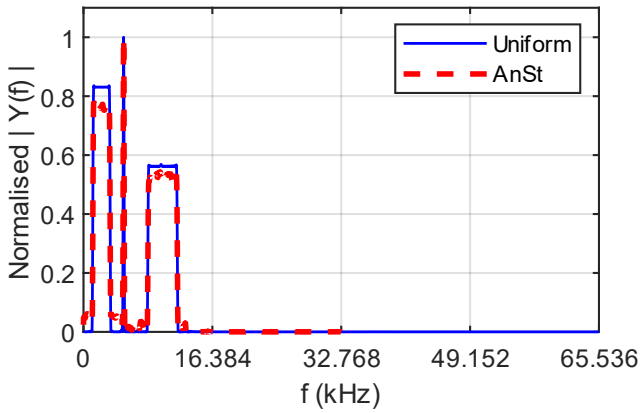

Fig. 10. The spectra of the filter outputs based on uniformly sampled (blue) and AnSt randomly sampled (dashed red) signals. Case 3) the filter input is a continuous signal with 500 bounded FOD discontinuities. F_{US}=131.072kHz, whereas F_{ARS}=65.536kHz.

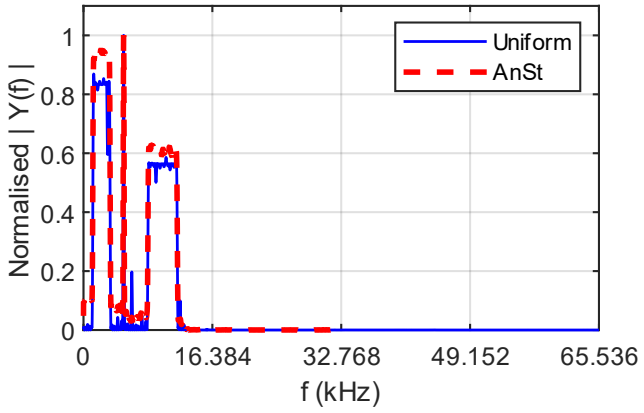

Fig. 11. The spectra of the filter outputs based on uniformly sampled (blue) and AnSt randomly sampled (dashed red) signals. Case 4) the filter input is a discontinuous signal with 250 bounded ZOD discontinuities. F_{US}=131.072kHz, whereas F_{ARS}=65.536kHz.

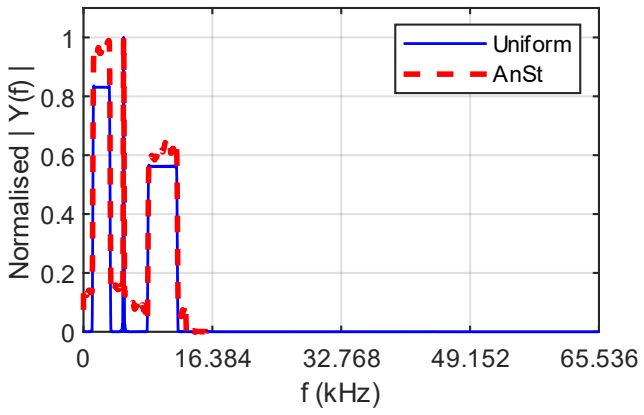

Fig. 12. The spectra of the filter outputs based on uniformly sampled (blue) and AnSt randomly sampled (dashed red) signals. The filter input is the same as that in Fig. 7, but unlike Case 1) of Fig. 8, the average random sampling frequency used here is only one quarter of the uniform sampling rate, i.e. F_{ARS}=32. 768kHz.

6. Conclusion

In this paper, we have demonstrated how to use the AnSt random sampling technique in a DASP-based filtering application. The proposed filter estimator is proven to be unbiased. However, this is only applicable for random sampling schemes with a uniform PDF and cannot be generalised for other types of distributions. Moreover, we have considered input signals that have finite number of bounded discontinuities in one or more orders of their derivatives. Having such discontinuities was found to be negatively affecting the variance of the estimator. If there are no discontinuities at all or the discontinuities only present in the SOD, then the rate of uniform convergence of the estimator, in these cases, is the fastest and it is exactly equal to N^{-5}. Whereas a rate of N^{-4} is achieved if the FOD is discontinuous, as well. Finally, for the case that the ZOD is also discontinuous, then the rate is proven to be the slowest, where only N^{-2} is reached. Although our estimator is based on equidistant stratification, it is also applicable for other nonuniform partitioning subject to some mild conditions already defined in the literature. The presented numerical examples verify the mathematical derivations and results.

Appendix A
Proof of Theorem 1

The expected value of $\hat{y}(t)$, given in (3), is

$$E[\hat{y}(t)] = E\left[\sum_{j=1}^{N}\left(g(t,\tau_j)+g(t,\tau_j^A)\right)\frac{\Delta_j}{2}\right], \tag{A.1}$$

$$E[\hat{y}(t)] = \sum_{j=1}^{N}\int_{-\infty}^{\infty} p_j(\tau)\left(g(t,\tau)+g(t,\tau^A)\right)\frac{\Delta_j}{2}\,d\tau, \tag{A.2}$$

$$\begin{aligned} E[\hat{y}(t)] &= \sum_{j=1}^{N}\int_{S_{j-1}}^{S_j}\frac{g(t,\tau)}{2}d\tau + \sum_{j=1}^{N}\int_{S_{j-1}}^{S_j}\frac{g(t,\tau^A)}{2}d\tau \\ &= \int_0^T \frac{g(t,\tau)}{2}d\tau - \sum_{j=1}^{N}\int_{2C_j-S_{j-1}}^{2C_j-S_j}\frac{g(t,\tau^A)}{2}d\tau^A \\ &= \frac{y(t)}{2} - \sum_{j=1}^{N}\int_{S_j}^{S_{j-1}}\frac{g(t,\tau^A)}{2}d\tau^A = \frac{y(t)}{2} - \left(-\frac{y(t)}{2}\right) \\ &= y(t). \end{aligned} \tag{A.3}$$

□

Appendix B
Proof of Theorem 2

From (12) and (13), we have

$$\begin{aligned} Var[Z_j] = \int_{S_{j-1}}^{S_j}\frac{1}{\Delta}\Big|&\frac{1}{4}\left(g''_{j,L}\left(\tau_{D_j}\right)+g''_{j,R}\left(\tau_{D_j}\right)\right)\left(\tau_j-\tau_{D_j}\right)^2\Delta - c_{2j}\,g''_{j,R}\left(\tau_{D_j}\right)\left(\tau_j-\tau_{D_j}\right)\Delta^2 + \\ &\frac{1}{12}\left(c_{3j}g''_{j,R}\left(\tau_{D_j}\right)-2K_j^3 g''_{j,L}\left(\tau_{D_j}\right)\right)\Delta^3+o(\Delta^3)\Big|^2 d\tau. \end{aligned} \tag{B.1}$$

$$Var[Z_j] = \frac{1}{720}\left(c_{4j}{G_{2j}}^2 + \left|g''_{j,L}\left(\tau_{D_j}\right) g''_{j,R}\left(\tau_{D_j}\right)\right|\right)\Delta^6 + o(\Delta^6), \quad \text{(B.2)}$$

with $c_{4j} = 9 - 45K_j + 90K_j^2 - 110K_j^3 + 105K_j^4 - 60K_j^5 + 20K_j^6$, and G_{2j} is defined in (6a), above.

Now, the variance of the whole N-strata AnSt-based filter estimator is

$$\begin{aligned} Var[\hat{y}] &= \sum_{j=1}^{N} Var[Z_j] \\ &= \frac{T^5}{720N^5}\sum_{j=1}^{N}\left(c_{4j}{G_{2j}}^2 + \left|g''_{j,L}\left(\tau_{D_j}\right) g''_{j,R}\left(\tau_{D_j}\right)\right|\right)\Delta \\ &+ o(N^{-5}). \end{aligned} \quad \text{(B.3)}$$

To check the uniform convergence rate of the estimator, we observe $Var[\hat{y}]$ as $N \to \infty$ by means of Riemann integration,

$$\begin{aligned} &\lim_{N\to\infty} N^5(\mathrm{Var}[\hat{y}]) \\ &= \lim_{N\to\infty}\left(\frac{T^5}{720}\sum_{j=1}^{N}\left(c_{4j}{G_{2j}}^2 + \left|g''_{j,L}\left(\tau_{D_j}\right) g''_{j,R}\left(\tau_{D_j}\right)\right|\right)\Delta\right). \end{aligned} \quad \text{(B.4)}$$

As the number of strata approaches infinity, $\Delta \to 0$. And since $g(\tau)$ is assumed to have an M number of SOD discontinuities, within the observation window, then $g''(\tau)$ will be a piecewise-continuous function with $M+1$ pieces. Though, it is still integrable, with the left and right SOD parts in (B.4) reduce to just $g''(\tau)$, because $g''_{j,L}\left(\tau_{D_j}\right) = g''_{j,R}\left(\tau_{D_j}\right)$ for all strata excluding the M ones with discontinuities. Hence, (B.4) can be calculated by adding $M+1$ integral terms,

$$\lim_{N\to\infty} N^5(Var[\hat{y}]) = \frac{T^5}{720}\sum_{k=1}^{M+1}\int_{T_{k-1}}^{T_k}\left(g''(\tau)\right)^2 d\tau. \quad \text{(B.5)}$$

□

Appendix C
Proof of Theorem 3

Evaluating the integrals in (10a), taking (16a)-(16c) into account, yields a new expression for the estimator's error in the j-th stratum, $E[Z_j]$,

$$\begin{aligned} E[Z_j] &= \frac{1}{6}\left(K_j^3 g''_{j,L}\left(\tau_{D_j}\right) - c_{1j}\, g''_{j,R}\left(\tau_{D_j}\right)\right)\Delta^3 \\ &+ c_{2j}\, g'_{j,R}\left(\tau_{D_j}\right)\Delta^2 - \frac{1}{2}K_j^2\, G_{1j}\,\Delta^2 + g_{j,R}\left(\tau_{D_j}\right)\Delta \\ &+ o(\Delta^3). \end{aligned} \quad \text{(C.1)}$$

To find the new j-th based sub-estimator error, in this case, we compute $e_j = Z_j - E[Z_j]$ using (8b) and (C.1). Again, we are interested in one of the four almost similar expressions for e_j, that is, when $\tau_j < \tau_{D_j} < \tau_j^A$.

$$\begin{aligned} e_j &= \frac{1}{2}\Delta\Bigg(2g_{j,R}\left(\tau_{D_j}\right) - g'_{j,L}\left(\tau_{D_j}\right)\left(\tau_{D_j} - \tau_j\right) \\ &- g'_{j,R}\left(\tau_{D_j}\right)\left(\tau_j - \tau_{D_j} + 2\Delta\left(K_j - \frac{1}{2}\right)\right) \\ &+ \frac{1}{2}g''_{j,L}\left(\tau_{D_j}\right)\left(\tau_{D_j} - \tau_j\right)^2 \\ &+ \frac{1}{2}g''_{j,R}\left(\tau_{D_j}\right)\left(\tau_j - \tau_{D_j} + 2\Delta\left(K_j - \frac{1}{2}\right)\right)^2\Bigg) \\ &+ \frac{1}{6}\Delta\left(-3\Delta g'_{j,R}\left(\tau_{D_j}\right)\left(K_j - 1\right)^2 + 6g_{j,R}\left(\tau_{D_j}\right)\left(K_j - 1\right)\right. \\ &\left. + \Delta^2 g''_{j,R}\left(\tau_{D_j}\right)\left(K_j - 1\right)^3\right) \\ &- \frac{1}{6}\Delta K_j\left(6g_{j,R}\left(\tau_{D_j}\right) - 3\Delta K_j g'_{j,L}\left(\tau_{D_j}\right)\right. \\ &\left. + \Delta^2 K_j^2 g''_{j,L}\left(\tau_{D_j}\right)\right) + o(\Delta^3). \end{aligned} \quad \text{(C.2)}$$

Now, the expected value of the estimator for one stratum is $Var[Z_j] = \int_{-\infty}^{\infty} p_j(\tau)\left|e_j\right|^2 d\tau = \Delta\int_{S_{j-1}}^{S_j}\left|e_j\right|^2 d\tau$. We include here the final answer since, algebraically, it is quite long, yet it is straight forward. Thus,

$$\begin{aligned} Var[Z_j] &= \frac{c_{5j}}{12}{G_{1j}}^2\Delta^4 + \frac{c_{6j}}{48}\left|G_{2j}G_{1j}\right|\Delta^5 + \frac{c_{7j}}{720}{G_{2j}}^2\Delta^6 \\ &+ \frac{1}{720}\left|g''_{j,L}\left(\tau_{D_j}\right) g''_{j,R}\left(\tau_{D_j}\right)\right|\Delta^6 + o(\Delta^6), \end{aligned} \quad \text{(C.3)}$$

where $c_{6j} = 2c_{2j}\left(3 - 6\,K_j + 10\,K_j^2 - 8\,K_j^3 + 4\,K_j^4\right)$, and $c_{7j} = c_{4j} + 20\,K_j^6$. For the N-strata AnSt-based filter estimator with a finite number, M, of bounded FOD and SOD discontinuities, we have,

$$\begin{aligned} Var[\hat{y}(t)] &= \sum_{j=1}^{N} Var[Z_j] \\ &= \sum_{j\in I_M}\left(\frac{c_{5j}}{12}{G_{1j}}^2\Delta^4 + \frac{c_{6j}}{48}\left|G_{2j}G_{1j}\right|\Delta^5 + \frac{c_{7j}}{720}{G_{2j}}^2\Delta^6\right) \\ &+ \frac{T^5}{720N^5}\sum_{\substack{n=1 \\ n\notin I_M}}^{N}\left|g''_{j,L}(\tau_{D_n})g''_{j,R}(\tau_{D_n})\right|\Delta + o(N^{-5}), \end{aligned} \quad \text{(C.4)}$$

$$\lim_{N\to\infty} N^4(\mathrm{Var}[\hat{y}(t)]) = \frac{T^4}{12}\sum_{j\in I_M} c_{5j}\,{G_{1j}}^2. \quad \text{(C.5)}$$

To distinguish between the two summations in (C.4), we have used different subscripts, j and n. Note that (C.5) proves that the variance of $\hat{y}(t)$ is converging at a uniform rate of N^{-4}, and this completes the proof of Theorem 3.

□

Appendix D
Proof of Theorem 4

We get an extra term in the expression of $E[Z_j]$ when recalculating the integrals in (10a) and considering (18a)- (18c),

$$
\begin{aligned}
&E[Z_j] \\
&= \frac{1}{6}\left(K_j^3 g''_{j,L}\left(\tau_{D_j}\right) - c_{1j}\, g''_{j,R}\left(\tau_{D_j}\right)\right)\Delta^3 \\
&+ c_{2j}\, g'_{j,R}\left(\tau_{D_j}\right)\Delta^2 - \frac{1}{2}K_j^2\, G_{1j}\,\Delta^2 + g_{j,R}\left(\tau_{D_j}\right)\Delta \\
&+ +K_j G_{0j}\Delta + o(\Delta^3).
\end{aligned} \tag{D.1}
$$

Analogous to the previous two sub-sections, we find the error term of the estimator in the j-th stratum, e_j, for the case when $\tau_j < \tau_{D_j} < \tau_j^A$. So, by subtracting (D.1) out from (8b) and simplifying the result algebraically, we get

$$
\begin{aligned}
&e_j \\
&= \frac{1}{2}\Delta\Bigg(2g_{j,R}\left(\tau_{D_j}\right) - g'_{j,L}\left(\tau_{D_j}\right)\left(\tau_{D_j} - \tau_j\right) \\
&- g'_{j,R}\left(\tau_{D_j}\right)\left(\tau_j - \tau_{D_j} + 2\Delta\left(K_j - \frac{1}{2}\right)\right) \\
&+ \frac{1}{2}g''_{j,L}\left(\tau_{D_j}\right)\left(\tau_{D_j} - \tau_j\right)^2 \\
&+ \frac{1}{2}g''_{j,R}\left(\tau_{D_j}\right)\left(\tau_j - \tau_{D_j} + 2\Delta\left(K_j - \frac{1}{2}\right)\right)^2\Bigg) \\
&+ \frac{1}{6}\Delta\left(-3\Delta g'_{j,R}\left(\tau_{D_j}\right)\left(K_j - 1\right)^2 + 6g_{j,R}\left(\tau_{D_j}\right)\left(K_j - 1\right)\right. \\
&\left.+ \Delta^2 g''_{j,R}\left(\tau_{D_j}\right)\left(K_j - 1\right)^3\right) \\
&- \frac{1}{6}\Delta K_j\left(6g_{j,R}\left(\tau_{D_j}\right) - 3\Delta K_j g'_{j,L}\left(\tau_{D_j}\right)\right. \\
&\left.+ \Delta^2 K_j^2 g''_{j,L}\left(\tau_{D_j}\right)\right) + o(\Delta^3).
\end{aligned} \tag{D.2}
$$

And the second moment of this error is equal to the sub-variance related to the j-th stratum, $Var[Z_j] = \Delta\int_{S_{j-1}}^{S_j}|e_j|^2 d\tau$,

$$
\begin{aligned}
&Var[Z_j] \\
&= {c_{2j}}^2\, {G_{0j}}^2\,\Delta^2 + \frac{1}{2}c_{2j}\, c_{8j}\,|G_{1j}G_{0j}|\Delta^3 \\
&+ \frac{1}{12}\left(c_{5j}\, {G_{1j}}^2 + 4{c_{2j}}^2 c_{9j}\,|G_{2j}G_{0j}|\right)\Delta^4 \\
&+ \frac{1}{48}c_{6j}\,|G_{2j}G_{1j}|\Delta^5 \\
&+ \frac{1}{720}\left(c_{4j}\, {G_{2j}}^2 + \left|g''_{j,L}\left(\tau_{D_j}\right) g''_{j,R}\left(\tau_{D_j}\right)\right|\right)\Delta^6 + o(\Delta^6),
\end{aligned} \tag{D.3}
$$

where $c_{8j} = 1 - 2K_j + 2K_j^2$ and $c_{9j} = 1 - K_j + K_j^2$.
The expected value of the filter estimator is simply the summation of the N individual sub-estimators. Hence,

$$
\begin{aligned}
&Var[\hat{y}(t)] = \sum_{j=1}^{N} Var[Z_j] = \sum_{j\in I_M}\left({c_{2j}}^2\, {G_{0j}}^2\,\Delta^2 + \right. \\
&\tfrac{1}{2}c_{2j}\, c_{8j}\,|G_{1j}G_{0j}|\Delta^3 + \tfrac{1}{12}\left(c_{5j}\, {G_{1j}}^2 + \right. \\
&\left.4{c_{2j}}^2 c_{9j}\,|G_{2j}G_{0j}|\right)\Delta^4 + \tfrac{1}{48}c_{6j}\,|G_{2j}G_{1j}|\Delta^5 + \\
&\left.\tfrac{1}{720}c_{4j}\, {G_{2j}}^2\,\Delta^6\right) + \tfrac{T^5}{720N^5}\sum_{\substack{n=1 \\ n\notin I_M}}^{N}\left|g''_{j,L}(\tau_{D_n})\, g''_{j,R}(\tau_{D_n})\right|\Delta + \\
&o(N^{-5}).
\end{aligned} \tag{D.4}
$$

$$
\lim_{N\to\infty} N^2\left(Var[\hat{y}(t)]\right) = T^2\sum_{j\in I_M}{c_{2j}}^2\, {G_{0j}}^2, \tag{D.5}
$$

It is obvious from (D.5) that the AnSt-based filter estimator is converging uniformly at an exact rate of N^{-2}. This completes the proof of Theorem 4.

□

References

[1] C. E. Shannon, 'Communication in the Presence of Noise', *Proc. IRE*, vol. 37, no. 1, pp. 10–21, Jan. 1949.

[2] H. Nyquist, 'Certain Topics in Telegraph Transmission Theory', *Trans. Am. Inst. Electr. Eng.*, vol. 47, no. 2, pp. 617–644, Apr. 1928.

[3] J. Yen, 'On Nonuniform Sampling of Bandwidth-Limited Signals', *IRE Trans. Circuit Theory*, vol. 3, no. 4, pp. 251–257, Dec. 1956.

[4] H. S. Shapiro and R. A. Silverman, 'Alias-Free Sampling of Random Noise', *J. Soc. Ind. Appl. Math.*, vol. 8, no. 2, pp. 225–248, 1960.

[5] E. Masry, 'Alias-free sampling: An alternative conceptualization and its applications', *IEEE Trans. Inf. Theory*, vol. 24, no. 3, pp. 317–324, May 1978.

[6] I. Bilinskis and A. K. Mikelson, *Randomized Signal Processing*. New York: Prentice Hall, 1992.

[7] I. Bilinskis, *Digital alias-free signal processing*. Chichester ; Hoboken, N.J: John Wiley, 2007.

[8] F. Marvasti, *Nonuniform Sampling: Theory and Practice*. Springer Science & Business Media, 2012.

[9] A. Tarczynski and N. Allay, 'Spectral analysis of randomly sampled signals: suppression of aliasing and sampler jitter', *IEEE Trans. Signal Process.*, vol. 52, no. 12, pp. 3324–3334, Dec. 2004.

[10] M. Al-Ani, A. Tarczynski, and B. I. Ahmad, 'A novel Fourier transform estimation method using random sampling', in *2011 19th European Signal Processing Conference*, Aug. 2011, pp. 859–863.

[11] B. I. Ahmad and A. Tarczynski, 'Spectral Analysis of Stratified Sampling: A Means to Perform Efficient Multiband Spectrum Sensing', *IEEE Trans. Wirel. Commun.*, vol. 11, no. 1, pp. 178–187, Jan. 2012.

[12] B. I. Ahmad and A. Tarczynski, 'A novel sub-Nyquist Fourier transform estimator based on alias-free hybrid stratified sampling', in *2016 IEEE International Conference on Acoustics, Speech and Signal Processing (ICASSP)*, Mar. 2016, pp. 4473–4477.

[13] M. Al-Ani, A. T. Tarczynski, and B. I. Ahmad, 'High-Order Hybrid Stratified Sampling: Fast Uniform-Convergence Fourier Transform Estimation', in *2018 52nd Asilomar Conference on Signals, Systems, and Computers*, Oct. 2018, pp. 1019–1023.

[14] A. Tarczynski, V. Valimaki, and G. D. Cain, 'FIR filtering of nonuniformly sampled signals', in *1997 IEEE International Conference on Acoustics, Speech, and Signal Processing*, Apr. 1997, vol. 3, pp. 2237–2240 vol.3.

[15] K. Kose and A. E. Cetin, 'Low-Pass Filtering of Irregularly Sampled Signals Using a Set Theoretic Framework [Lecture Notes]', *IEEE Signal Process. Mag.*, vol. 28, no. 4, pp. 117–121, Jul. 2011.

[16] W. B. Ye and Y. J. Yu, ‘An efficient FIR filtering technique for processing non-uniformly sampled signal’, in *2015 IEEE International Conference on Digital Signal Processing (DSP)*, Jul. 2015, pp. 182–186.

[17] H. Y. Darawsheh and A. Tarczynski, ‘Filtering Nonuniformly Sampled Grid-Based Signals’, in *2018 4th International Conference on Frontiers of Signal Processing (ICFSP)*, Sep. 2018, pp. 56–60.

[18] A. E. G. Huber and S.-C. Liu, ‘Filtering of Nonuniformly Sampled Bandlimited Functions’, *IEEE Signal Process. Lett.*, vol. 26, no. 7, pp. 1036–1040, Jul. 2019.

[19] H. Y. Darawsheh and A. Tarczynski, ‘Comparison Between Uniform and Nonuniform Interpolation Techniques for Digital Alias-free FIR Filtering’, in *International Conference on Digital Image & Signal Processing (DISP’19)*, Oxford, United Kingdom, May 2019, pp. 1–5.

[20] H. Y. Darawsheh and A. Tarczynski, ‘FIR Filtering of Discontinuous Signals: A Random-Stratified Sampling Approach’, in *ICASSP 2020 - 2020 IEEE International Conference on Acoustics, Speech and Signal Processing (ICASSP)*, May 2020, pp. 5800–5804.

[21] A. Tarczynski and H. Y. Darawsheh, ‘DASP Implementation of Continuous-Time, Finite-Impulse-Response Systems’, in *’2020 28th European Signal Processing Conference (EUSIPCO)*, Amsterdam, the Netherlands, Jan. 2021, pp. 2244–2248.

[22] F. Esqueda, S. Bilbao, and V. Välimäki, ‘Aliasing Reduction in Clipped Signals’, *IEEE Trans. Signal Process.*, vol. 64, no. 20, pp. 5255–5267, Oct. 2016.

[23] S. R. Baker, N. Bloom, S. J. Davis, K. Kost, M. Sammon, and T. Viratyosin, ‘The Unprecedented Stock Market Reaction to COVID-19’, *Rev. Asset Pricing Stud.*, no. raaa008, Jul. 2020.

[24] E. Masry, ‘Random sampling of deterministic signals: statistical analysis of Fourier transform estimates’, *IEEE Trans. Signal Process.*, vol. 54, no. 5, pp. 1750–1761, May 2006.

[25] E. Masry and A. Vadrevu, ‘Random Sampling Estimates of Fourier Transforms: Antithetical Stratified Monte Carlo’, *IEEE Trans. Signal Process.*, vol. 57, no. 1, pp. 194–204, Jan. 2009.